# Tensile properties of mechanically alloyed oxide dispersion strengthened iron alloys Part 1 – Neural network models

A. Y. Badmos, H. K. D. H. Bhadeshia, and D. J. C. MacKay

*A neural network technique trained within a Bayesian framework has been applied to the analysis of the yield strength, ultimate tensile strength, and percentage elongation of mechanically alloyed oxide dispersion strengthened ferritic steels. The database used was compiled using information from the published literature, consisting of variables known to be important in influencing mechanical properties. The analysis has produced patterns which are metallurgically reasonable, and which permit the quantitative estimation of mechanical properties together with an indication of confidence limits.* *MST/3791*

*At the time the work was carried out Dr Badmos and Dr Bhadeshia were in the Department of Materials Science and Metallurgy, University of Cambridge. Dr Badmos is now in the Department of Chemical and Materials Engineering, University of Alberta, Edmonton, Canada. Dr MacKay is in the Cavendish Laboratory, University of Cambridge.* *Manuscript received 26 March 1997; in final form 15 May 1997.*


## Introduction

Mechanical alloying provides a technique for the production of dispersion strengthened alloys having interesting chemical compositions and unique properties. The process consists of blending elemental powders with master alloy powders in an attritor, and ball milling the mixture under a dry and protective atmosphere. The resulting alloyed powder is highly cold worked and can be homogeneous in its microstructure.[1] On completion of mechanical alloying, the powder is canned, extruded, and hot rolled to bars or hot and cold rolled to sheet.

Mechanically alloyed oxide dispersion strengthened (MA-ODS) alloys are already available in commercial quantities. The technique is nevertheless somewhat unusual and a large number of important phenomena are not yet understood. Experimental measurements of the mechanical properties of the alloys, for example, have not been systematically coordinated to reveal a definite pattern with respect to the numerous variables thought to be important in understanding the service behaviour of the alloys. The objective of the present work was to investigate whether an artificial neural network[2] could be trained to predict the ultimate tensile strength, yield strength, and elongation of MA-ODS ferritic steels as a non-linear function of these variables. In Table 1 the chemical compositions are given of some commercial MA-ODS steels which are most represented in the data used for the present analysis.[3–11]

This paper is presented first with an introduction to the method, followed by a description of the process by which the optimum model was obtained in each instance. The final section is concerned with the use of the models to ensure that the perceived relationships are metallurgically significant.

## Technique

Most workers are familiar with regression analysis, where data are 'best fitted' to a specified relationship which is usually linear. The result is an equation in which each of the inputs $x_j$ is multiplied by a weight $w_j$. The sum of all such products and a constant $\theta$ then gives an estimate of the output $y = \Sigma_j w_j x_j + \theta$. It is well understoood that there are dangers in using such relationships beyond the range of fitted data.

A neural network is a more general method of regression analysis. As before, the input data $x_j$ are multiplied by weights, but the sum of all these products forms the argument of a hyperbolic tangent. The output $y$ is therefore a non-linear function of $x_j$, the function usually selected being the hyperbolic tangent because of its flexibility. The exact shape of the hyperbolic tangent can be varied by altering the weights (Fig. 1*a*). Further degrees of non-

**Table 1 Chemical composition of some commercial MAODS steels, wt-%**

| Steel | Cr | Al | Mo | Ti | $Y_2O_3$ | Fe |
|---|---|---|---|---|---|---|
| MA956 | 20·0 | 4·5 | ... | 0·5 | 0·5 | Bal. |
| MA957 | 14·0 | ... | 0·3 | 1·0 | 0·27 | Bal. |
| DY (DT2203Y05) | 13·0 | ... | 1·5 | 2·2 | 0·5 | Bal. |
| DT (DT2906) | 13·0 | ... | 1·5 | 2·9 | ... | Bal. |

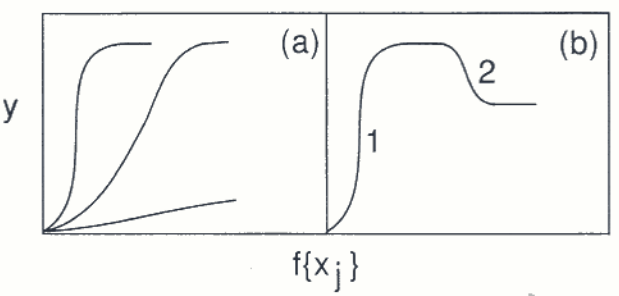


**1 *a* three different hyperbolic tangent functions – 'strength' of each depends on weight, and *b* combination of two hyperbolic tangents to produce more complex model**

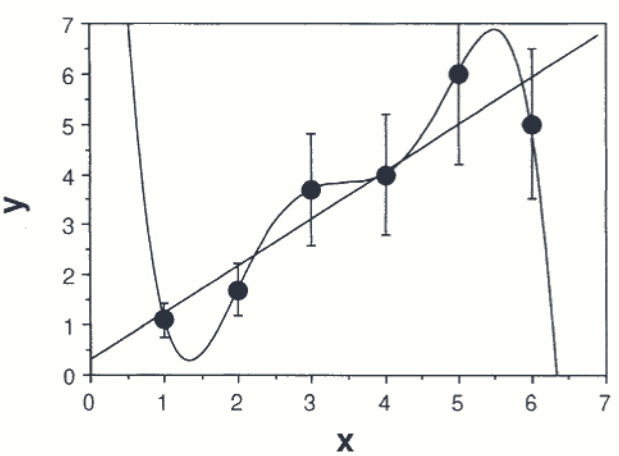


**2 Complex model shown may fit data, but in this instance a linear relationship may be all that is justified by noise in data**

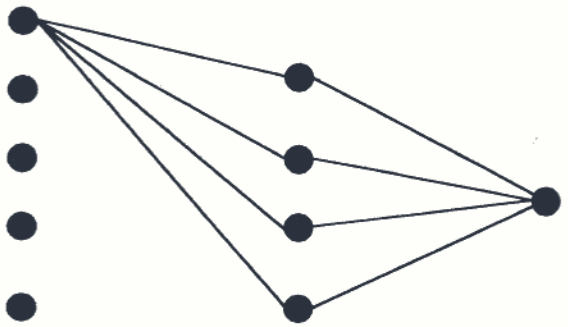


**3 Typical network used in analysis: connections originating from only one input unit are illustrated and two bias units are not illustrated**

linearity can be introduced by combining several of these hyperbolic tangents (Fig. 1*b*), so that the neural network method is able to replicate almost arbitrarily non-linear relationships. It is well known that the effect of chromium on the microstructure of steels is markedly different at high concentrations than in dilute alloys. Ordinary regression analysis cannot cope with such changes in the form of relationships.

A neural network is 'trained' using a set of examples of input and output data. The outcome of the training is a set of coefficients (weights) and a specification of the functions which in combination with the weights relate the input to the output. The training process involves a search for the optimum non-linear relationship between the input and the output data and is computer intensive. Once the network is trained, estimation of the outputs for any given inputs is very rapid.

One of the difficulties associated with blind data modelling is that of 'overfitting', in which spurious details and noise in the training data are overfitted by the model (Fig. 2). This results in solutions that generalise poorly. MacKay[12–16] has developed a Bayesian framework for neural networks in which the appropriate model complexity is inferred from the data.

The Bayesian framework for neural networks has two further advantages. First, the significance of the input variables is automatically quantified. Consequently the significance, perceived by the model, of each input variable can be compared against metallurgical theory. Second, the predictions of the network are accompanied by error bars which depend on the specific position in input space. These quantify the certainty of the model regarding its predictions.

The neural network method has recently been applied to many materials problems, for example: the impact toughness of C–Mn steel arc welds by Bhadeshia *et al.*;[17] an analysis of the strength of nickel base superalloys by Jones and MacKay;[18] austenite formation in steels by Gavard *et al.*;[19] yield and ultimate tensile strength of steel welds by Cool *et al.*;[20] fatigue crack growth rate in nickel base superalloys by Fujii *et al.*;[21] mechanical properties in the heat affected zone of power plant steels by Cool and Bhadeshia;[22] prediction of martensite start temperature by

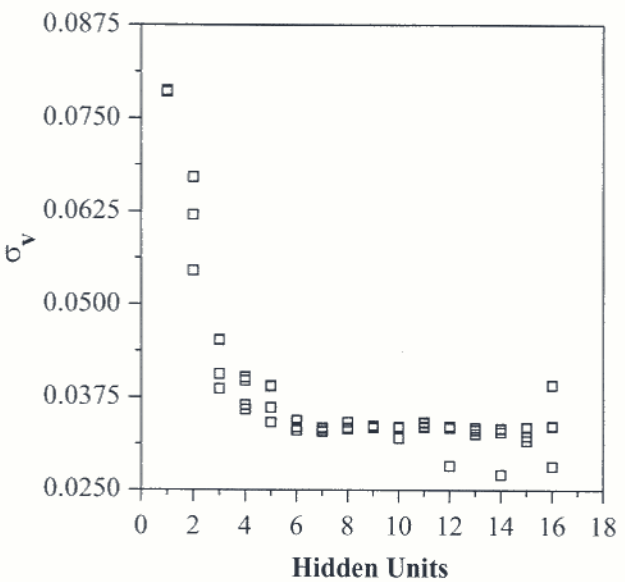


**4 Yield strength analysis: variation in model perceived noise level $\sigma_v$ as function of number of hidden units (i.e. complexity of model) – several values are presented for each set of hidden units because training for each network was started with various random seeds**

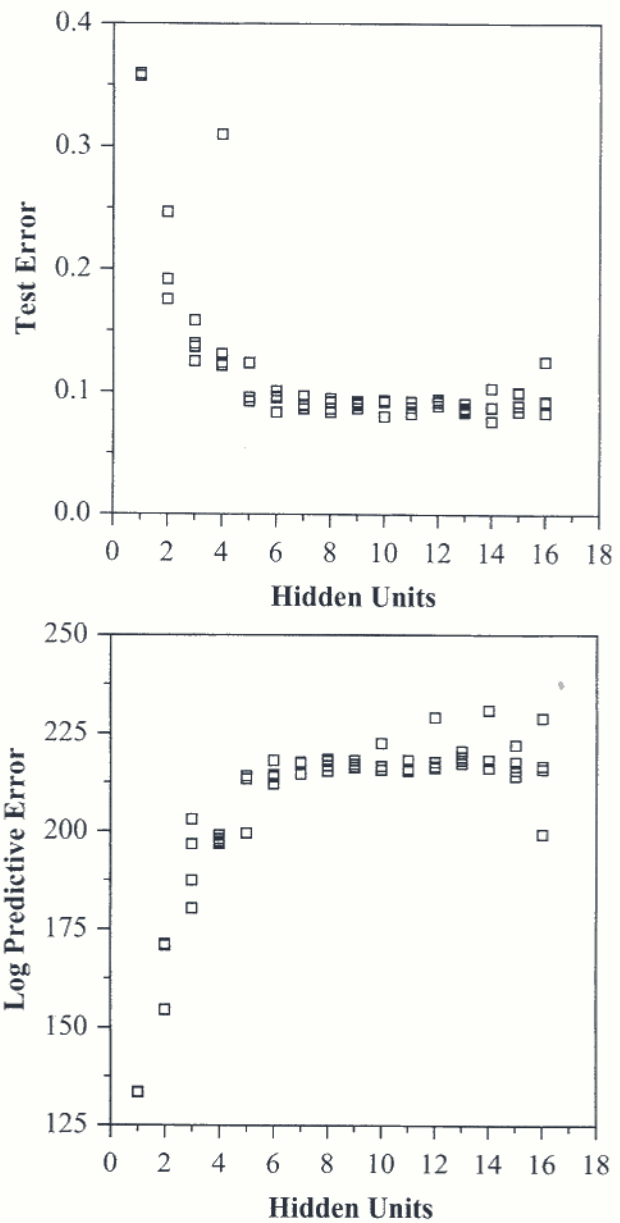


**5 Yield strength analysis: variation in test error and log predictive error as functions of number of hidden units – note that larger log predictive error indicates superior model**

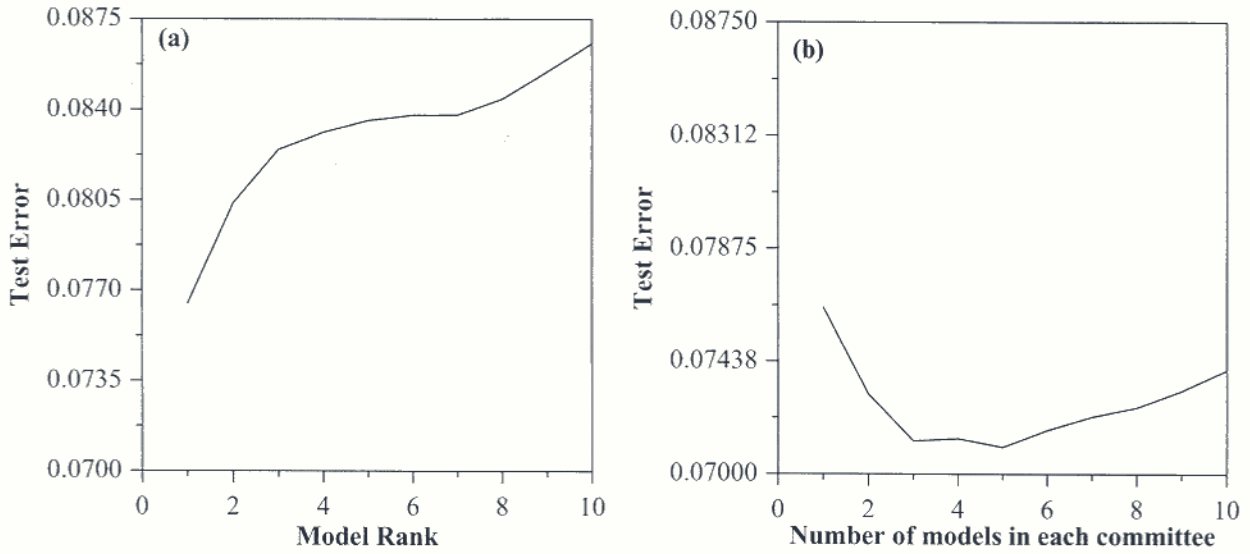


**6** *a* test errors of top 10 yield strength models, and *b* corresponding test errors for committee models

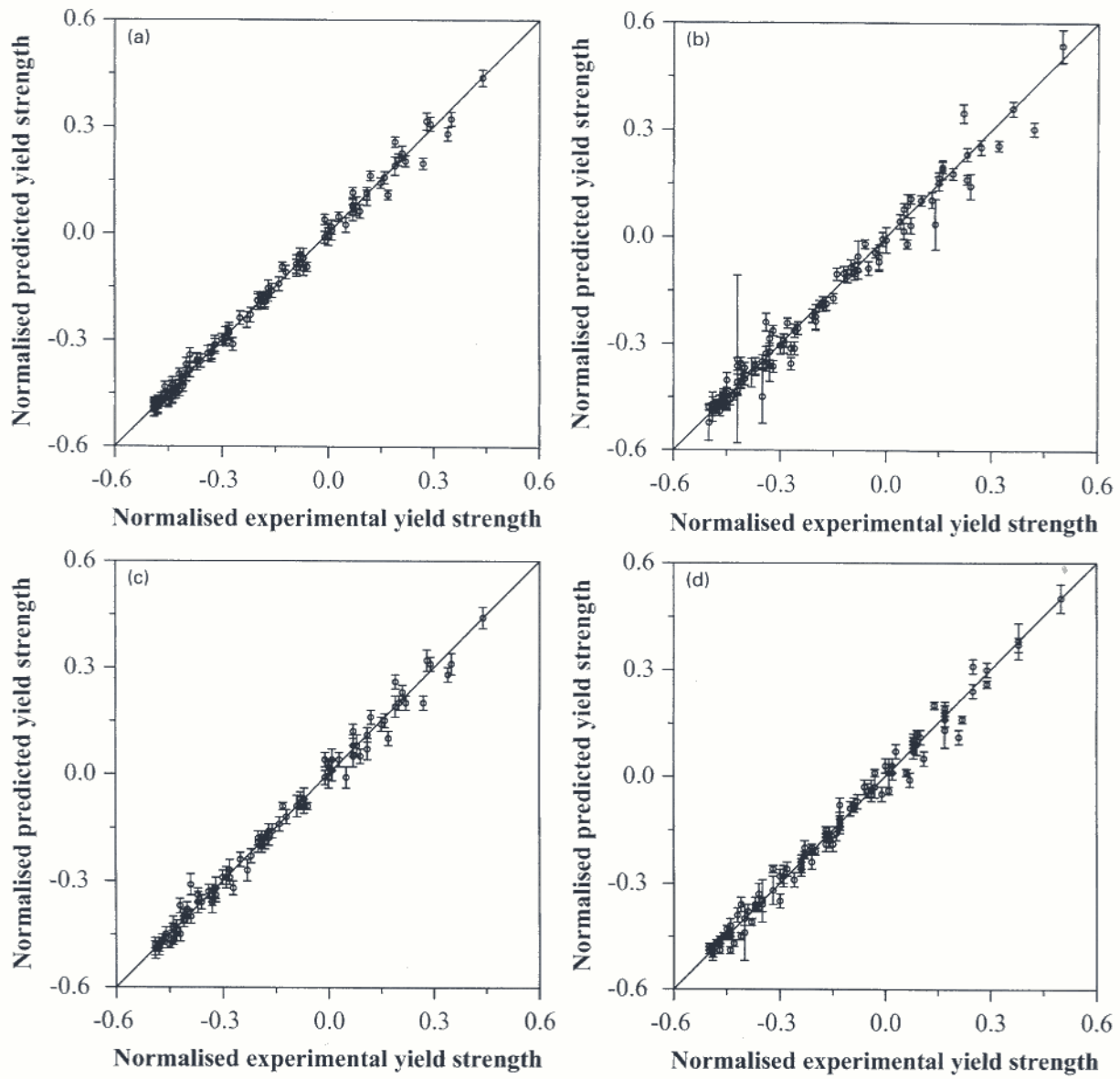


*a* single model, training data set; *b* single model, test data set; *c* committee, training data set; *d* committee, test data set

**7** Normalised predicted yield strength versus normalised experimental results using *a*, *b* single best model and *c*, *d* optimum committee

Vermeulen *et al.*;[23] prediction of the continuous cooling transformation diagram of some selected steels by Vermeulen *et al.*;[24] and prediction of the measured temperature after the last finishing stand in hot rolling by Vermeulen *et al.*[25]

## Analysis

Both the input and output variables were normalised within the range +0·5 to −0·5. The normalisation is obtained through a procedure which is expressed quantitatively as

$$x_N = \frac{x - x_{min}}{x_{max} - x_{min}} - 0{\cdot}5 \quad . . . . . (1)$$

where $x_N$ is the normalised value of $x$, which has the minimum and maximum values given by $x_{min}$ and $x_{max}$ respectively. The normalisation is not necessary for the analysis but it facilitates the subsequent comparison of the significance of each of the variables.

Figure 3 shows a typical network. Each network consists of input nodes (one for each variable $x$), a number of hidden nodes, and an output node. Linear functions of the inputs $x_j$ are operated on by a hyperbolic tangent transfer function

$$h_i = \tanh\left(\sum_j w_{ij}^{(1)} x_j + \theta_i^{(1)}\right) \quad . . . . . (2)$$

so that each input contributes to every hidden unit. The bias is designated $\theta_i$ and is analogous to the constant that appears in linear regression analysis. The strength of the transfer function is in each case determined by the weight $w_{ij}$. The transfer to the output $y$ is linear

$$y = \sum_i w_{ij}^{(2)} h_i + \theta^{(2)} \quad . . . . . (3)$$

The specification of the network structure, together with the set of weights, is a complete description of the formula relating the input to the output. The weights are determined by training the network. The training is carried out using a data set $D = \{x^{(m)}, t^{(m)}\}$ by adjusting the weights $w$ to minimise an error function, e.g.

$$E_D(w) = \frac{1}{2}\sum_m \sum_i [t_i^{(m)} - y_i(x^{(m)}; w)]^2 \quad . . . . . (4)$$

This objective function is a sum of terms, one for each input–target pair $\{x, t\}$, measuring the degree of correlation between the output $y\{x; w\}$ and the target $t$ (Ref. 16). The parameter $m$ denotes each input–output pair.

The training for each network is started with a variety of random seeds. The value of a term $\sigma_v$ gives the framework estimate of the overall noise level of the data. The complexity of the model is controlled by the number of hidden units and the values of the regularisation constants ($\sigma_w$), one associated with each of the inputs, one for biases, and one for all weights connected to the output. The noise level decreases monotonically as the number of hidden units increases. However, the complexity of the model also increases with the number of hidden units. A high degree of complexity may not be justified if the model attempts to fit the noise in the experimental data. MacKay[12,13,15,16] has made a detailed study of this problem and defined a quantity (the 'evidence') which acts as an indicator of the probability of a model. In circumstances where two models give similar results for the known data set, the more probable model would be predicted to be that which is simpler; this simple model would have a higher value of evidence. The evidence framework is used to control the regularisation constants and $\sigma_v$. The number of hidden units is set by examining performance on test data. A combination of Bayesian and pragmatic statistical techniques is therefore used to control the complexity of the model. A further procedure used to avoid the overfitting problem was to divide the experimental data randomly into two equal sets, namely, the training and test data sets. The models are developed using the training data only. The unseen test data are then used to assess how well the model generalises. A good model would produce similar levels of error in both the test and training data whereas an overfitted model might accurately predict the training data but badly estimate the unseen test data. Once the correct complexity of the model has been determined using this procedure, it can be retrained using all the data with a small but significant reduction in the error.

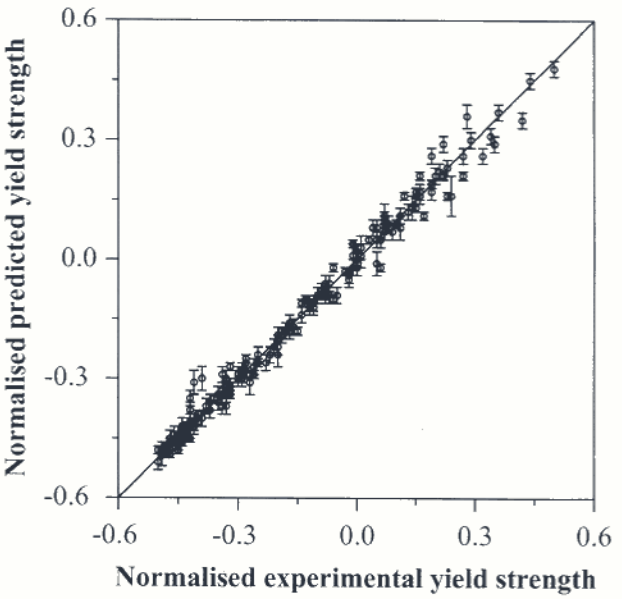


**8 Normalised predicted yield strength versus normalised experimental results for whole data set after retraining using optimum committee**

**Table 2 Variables used in analysis of yield strength**

| Variable | Range | Mean | Standard deviation |
|---|---|---|---|
| Chromium, wt-% | 13–20 | 17·30 | 3·20 |
| Aluminium, wt-% | 0–4·5 | 2·62 | 2·23 |
| Titanium, wt-% | 0·5–3·50 | 1·03 | 0·86 |
| Molybdenum, wt-% | 0–1·5 | 0·35 | 0·56 |
| Yttria, wt-% | 0–0·5 | 0·41 | 0·15 |
| Recrystallisation temperature, °C | 20–1330 | 697 | 595 |
| Recrystallisation time, s | 0–120 | 28·44 | 33·38 |
| Aging temperature, °C | 20–800 | 163·3 | 303 |
| Aging time, s | 0–2888 | 327 | 739 |
| Cold work, % | 0–70 | 10·43 | 19·64 |
| Test temperature, °C | 0–1200 | 562·1 | 340·4 |
| Strain rate, $s^{-1}$ | $3 \times 10^{-8}$–$3 \times 10^{-2}$ | $9{\cdot}89 \times 10^{-4}$ | $2{\cdot}5 \times 10^{-3}$ |
| Yield strength, MPa | 63–1600 | 497 | 388 |

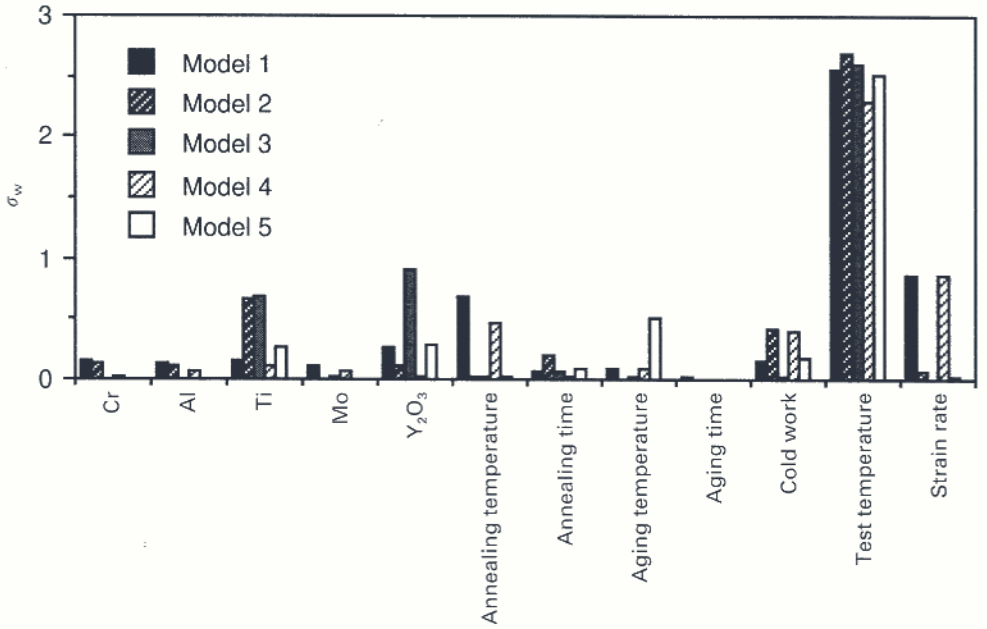


**9 Model perceived significance of input parameters for committee model trained on all yield strength data; $\sigma_w$ values for all members of committee are presented for each variable**

The test error $T_{en}$ is a reflection of the ability of the model to predict the target values in the test data

$$T_{en} = 0{\cdot}5 \sum_{n} (y_n - t_n)^2 \quad \ldots\ldots\ldots\ldots\ldots\ldots (5)$$

where $y_n$ is the set of predictions made by the model, and $t_n$ the corresponding target (experimental) values previously unseen by the model.

It is popular to use the test error (sum squared error) as the default performance measure whereby the model with the lowest test error is considered to be the best.[16] In many applications there will be an opportunity to make a prediction with error bars rather than a simple scalar prediction, or maybe to carry out an even more complex predictive procedure. It is then reasonable to compare models in terms of their predictive performance as measured by the log predictive probability of the test data. Under the log predictive error, as contrasted with the test error, the penalty for making a 'wild' prediction is much less if the wild prediction is accompanied by appropriately large error bars. Assuming that for each example $m$ the model gives a prediction with error $(y^{(m)}, \sigma^{(m)^2})$, the log predictive error (LPE) is

$$\mathrm{LPE} = \sum_{m} \left\{ \frac{1}{2}(t^{(m)} - y^{(m)})^2 \Big/ \sigma_y^{(m)^2} + \log[(2\pi)^{1/2}\sigma_y^{(m)}] \right\} \quad \ldots\ldots\ldots (6)$$

When making predictions, MacKay[16] has recommended the use of multiple good models instead of just one best model. This is termed 'forming a committee'. The committee prediction $\bar{y}$ is obtained using the expression

$$\bar{y} = \frac{1}{L} \sum_{i} y_i \quad \ldots\ldots\ldots\ldots\ldots\ldots\ldots (7)$$

where $L$ is the size of the committee and $y_i$ is the estimate of a particular model $i$. The optimum size of the committee is determined from the validation error of the committee's predictions using the test data set. The test error of the predictions made by a committee is calculated by replacing the $y_n$ in equation (5) with $\bar{y}$.

**Table 3 Ranking by test error of 10 best models of yield strength**

| Ranking | Hidden units | Seed | Test error | Log predictive error |
|---|---|---|---|---|
| 1 | 14 | 100 | 0·0764770 | 230·75 |
| 2 | 10 | 100 | 0·080370 | 222·37 |
| 3 | 11 | 100 | 0·082443 | 217·96 |
| 4 | 16 | 30 | 0·083116 | 228·67 |
| 5 | 6 | 30 | 0·083576 | 218·03 |
| 6 | 8 | 100 | 0·083781 | 217·81 |
| 7 | 13 | 10 | 0·083790 | 220·32 |
| 8 | 15 | 30 | 0·084411 | 221·84 |
| 9 | 13 | 100 | 0·085464 | 218·76 |
| 10 | 6 | 10 | 0·086566 | 218·26 |

**Table 4 Test errors of committees organised for estimation of yield strength: note that test error of best committee is less than that of single best model**

| Number of models in committee | Test error |
|---|---|
| 1 | 0·07648 |
| 2 | 0·07309 |
| 3 | 0·07128 |
| 4 | 0·07137 |
| 5 | 0·07104 |
| 6 | 0·07170 |
| 7 | 0·07221 |
| 8 | 0·07257 |
| 9 | 0·07322 |
| 10 | 0·07403 |

## Yield strength model

The technique was applied to the variables given in Table 2 for the analysis of the yield strength. There were 232 data, 12 input variables, and one output which is the yield strength. The major alloying elements (chromium, aluminium, titanium, and molybdenum) are expected to influence the yield strength primarily via solid solution strengthening. In some alloys molybdenum, titanium, and chromium also precipitate as an intermetallic compound, $\chi$ phase (FeCrTiMo) after a low temperature aging treatment.[8] Yttrium oxide is present as a very fine dispersion and must enhance strength at all temperatures by impeding the glide of dislocations. The recrystallisation heat treatment has a very severe effect on the microstructure since it changes an ultrafine primary recrystallised grain structure to a structure that is coarse and columnar. Cold work is naturally

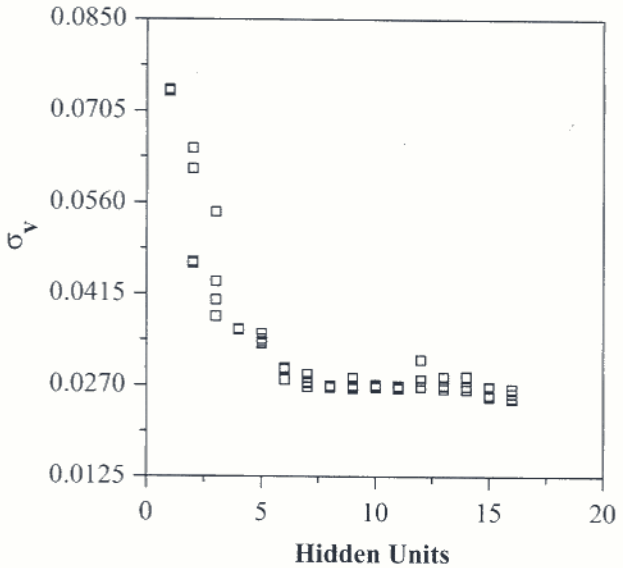


**10 Ultimate tensile strength analysis: variation in model perceived noise level $\sigma_v$ as function of hidden units (i.e. complexity of model) – several values are presented for each set of hidden units because training for each network was started with various random seeds**

expected to increase the yield strength; the data set included a variety of methods of cold deformation including rolling and swaging. The yield strength of body centred cubic metals is particularly sensitive to temperature because of the large Peierls barriers to dislocation motion. A further temperature dependence originates from the possibility of the climb of dislocations over dispersoids. There may in unrecrystallised alloys be an additional effect due to the onset of dynamic recrystallisation.

The plot of $\sigma_v$ as a function of the complexity of the models is shown in Fig. 4. Note that a number of values are presented for each hidden unit because the training process was started using different randomly selected seeds which determine the starting values of the weights. The test error and log predictive error versus number of hidden units are shown in Fig. 5.

The numerical data for the top ten models ranked by their test error are given in Table 3. Table 4 gives the test errors of the ten committees formed, starting with the best model and progressively increasing the number of models in the committee. The plots of the test errors of the top ten models and those of the committees are shown in Fig. 6 plotted on the same scale to show the usual reduction in test error when an appropriate committee is formed. The committee consisting of five top ranking models has the least test error and was used for the study of the yield strength presented below.

The plots of the predicted values versus experimental values using the training and test data sets for the single best model and the committee are shown in Fig. 7. Figure 8 shows the plot for the committee after retraining using the whole data set.

The significance of each of the input variables perceived by the various models contained in the committee is shown by $\sigma_w$ in Fig. 9. The parameter $\sigma_w$ is rather like a partial correlation coefficient in that it represents the amount of variation in the output that can be attributed to any particular input parameter and does not necessarily represent the sensitivity of the output to each of the inputs. As expected, the yield strength correlates strongly with temperature.

## Ultimate tensile strength

The neural network technique was applied to the ultimate tensile strength (UTS) data given in Table 5. The variables are identical to those used for the yield strength analysis. It would ideally be of interest to include the strain hardening coefficient since this determines the plastic instability which defines the ultimate strength. However, no such data could be found in the published literature. There were 12 input variables and one output variable, the ultimate tensile strength. A total of 232 data were used. As before, the data were divided equally and randomly into test and training data sets, the training data set being used to train the model and the ability of the model to generalise being examined by checking its performance on the unseen test data.

Figure 10 shows the plot of $\sigma_v$ versus hidden units. As expected, the inferred noise level decreases monotonically as the number of hidden units increases.

Figure 11 shows the variation of test error and log predictive error as functions of the number of hidden units. The calculated test error reaches a minimum at 16 hidden units and the log predictive error also exhibits a maximum at the same number of hidden units. This would have been the optimum model had a single model been used for the analysis.

A committee model was used. Based on the values of the test error and log predictive error, four models were selected as the best. The models were ranked using their test error values as presented in Table 6.

The optimum number of models in the committee was determined from the calculated validation errors of the different possible committees. Figure 12 shows the variation of the test error of the best models as a function of their position on the ranking table and the test error of the committees as a function of the number of models. It is evident that forming a committee reduces the test error, and hence improves predictions.

As shown in Fig. 12 the committee consisting of the top three models shows the least test error and was used

**Table 5 Variables used in analysis of ultimate tensile strength (UTS)**

| Variable | Range | Mean | Standard deviation |
|---|---|---|---|
| Chromium, wt-% | 13–20 | 17·19 | 3·22 |
| Aluminium, wt-% | 0–4·5 | 2·54 | 2·24 |
| Titanium, wt-% | 0·5–3·50 | 1·1 | 0·87 |
| Molybdenum, wt-% | 0–1·5 | 0·37 | 0·58 |
| Yttria, wt-% | 0–0·5 | 0·41 | 0·15 |
| Recrystallisation temperature, °C | 20–1330 | 684 | 594 |
| Recrystallisation time, s | 0–120 | 27·56 | 33·24 |
| Aging temperature, °C | 20–800 | 174·7 | 311·7 |
| Aging time, s | 0–2888 | 361 | 781 |
| Cold work, % | 0–70 | 10·47 | 19·71 |
| Test temperature, °C | 0–1200 | 561·1 | 347·6 |
| Strain rate, $s^{-1}$ | $3 \times 10^{-8}$–$3 \times 10^{-2}$ | $1{\cdot}1 \times 10^{-3}$ | $2{\cdot}5 \times 10^{-3}$ |
| UTS, MPa | 70·7–1680 | 575·3 | 407·3 |

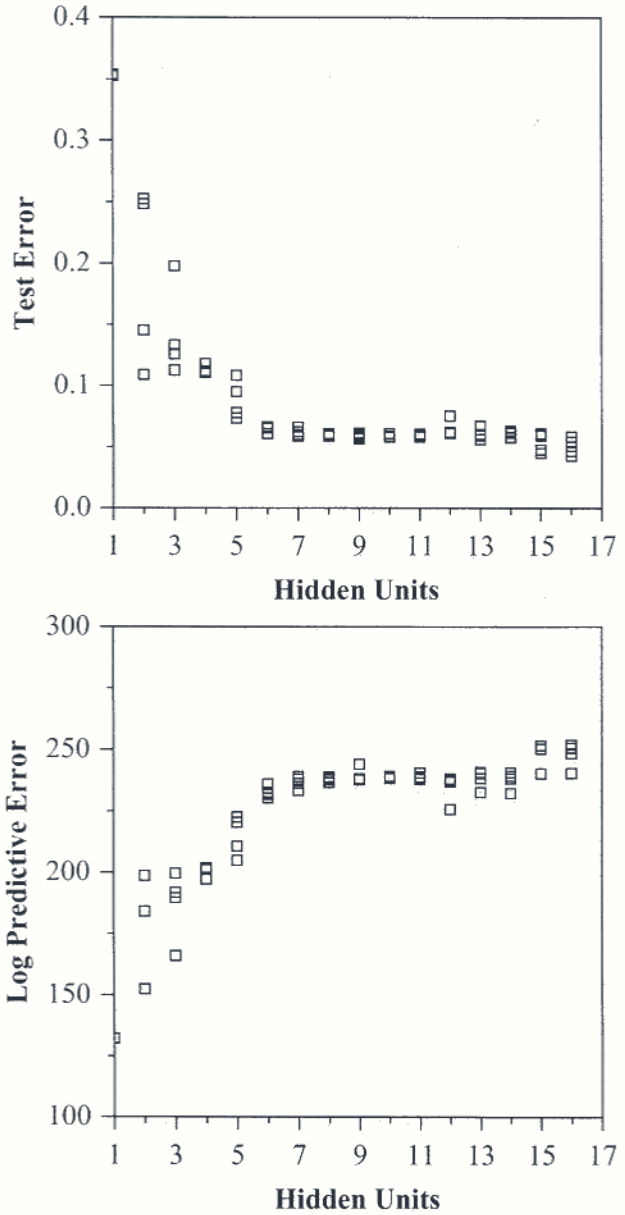


**11 Ultimate tensile strength analysis: variation in test error and in log predictive error as functions of number of hidden units – note that larger log predictive error indicates superior model**

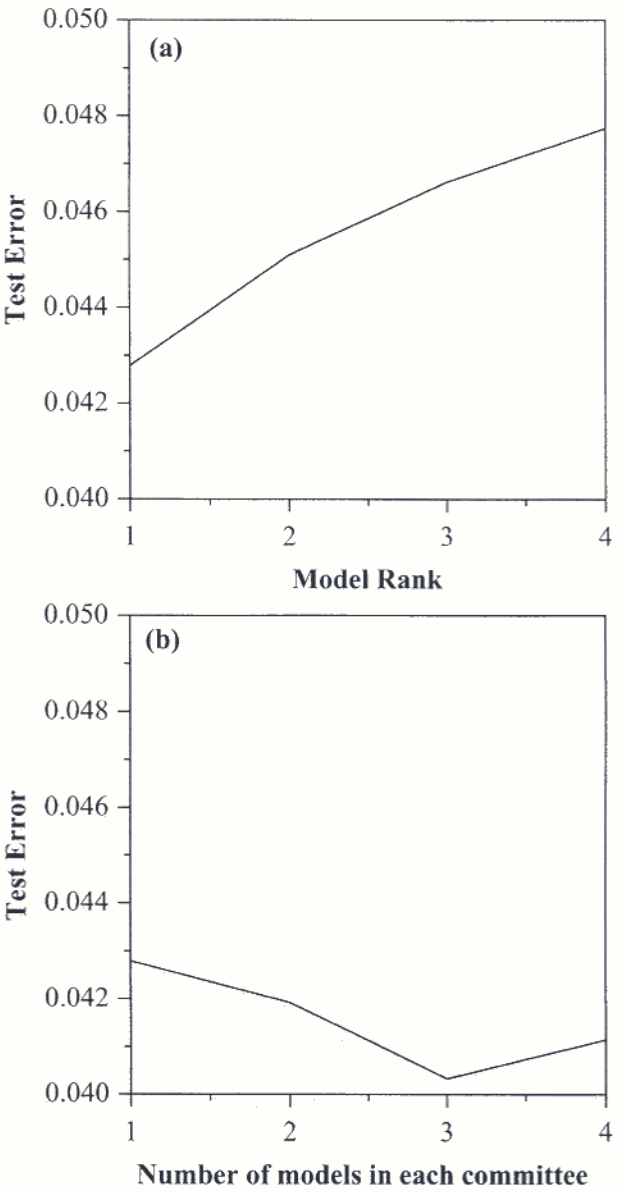


**12 *a* test error of four best ultimate tensile strength models and *b* corresponding test errors for committees of models**

for the analysis. The agreement between the predicted and experimental values for the training and test data sets is shown in Fig. 13 for the single best model and the committee.

The committee models were then retrained on the whole data set starting with the weights determined from the previous training exercise. Figure 14 shows the plot of the predicted values versus experimental values for the whole data set after the retraining. The retraining is shown to have significantly improved the model with the reduction in error bars and the apparent absence of outliers.

**Table 6 Ranking according to test error for four best models of ultimate tensile strength**

| Ranking | Hidden units | Seed | Test error | Log predictive error |
|---|---|---|---|---|
| 1 | 16 | 30 | 0·042786 | 250·73 |
| 2 | 15 | 30 | 0·045090 | 250·15 |
| 3 | 16 | 100 | 0·046607 | 250·49 |
| 4 | 15 | 100 | 0·047735 | 251·45 |

The significance of each of the input variables perceived by the various models contained in the committee is shown by $\sigma_w$ in Fig. 15. The test temperature is shown to have the largest $\sigma_w$ for all three models in the committee. This shows that the models have recognised a pattern correctly because temperature is more widely varied than any other input in the database. Moreover, temperature is known to affect strength very significantly.

## Elongation model

The ultimate tensile strength and yield strength were included as input variables in addition to the 12 input variables used in the strength analysis (Table 7). The inclusion of the strength parameters became necessary after the initial attempts to train the network without these parameters failed to produce acceptable results. The reason for this behaviour is obvious, in that the ductility of a material is a function of strength. The database consists of 232 examples and the noise level in the data is as plotted in Fig. 16*a*.

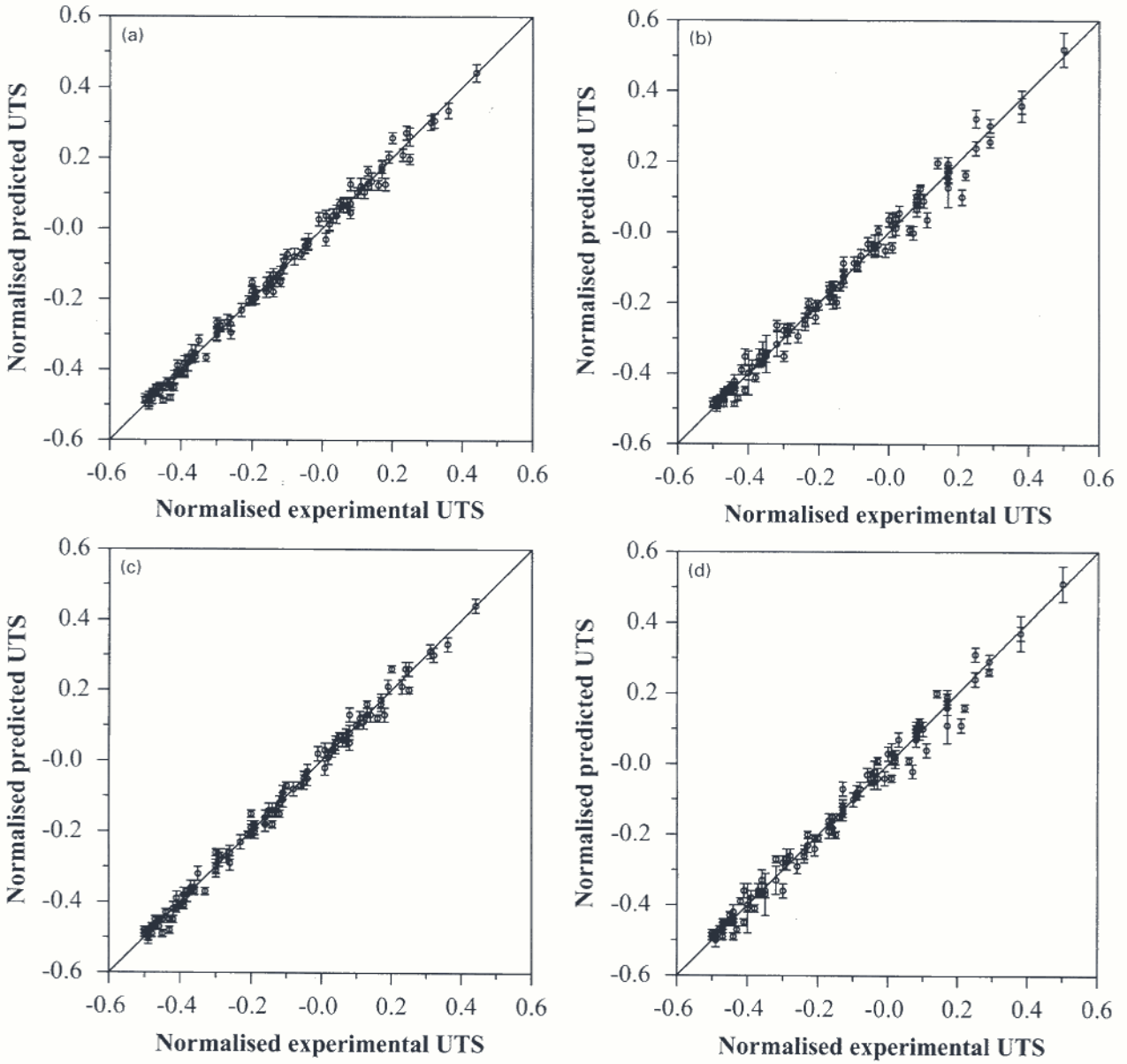


*a* single model, training data set; *b* single model, test data set; *c* committee, training data set; *d* committee, test data set

**13 Normalised predicted ultimate tensile strength versus normalised experimental results using *a*, *b* single best model and *c*, *d* optimum committee**

Test error and log predictive error as functions of hidden units are shown in Fig. 16*b* and *c*.

The numerical data for the ten best models ranked according to their log predictive errors are given in Table 8. Although the ranking of the models was by their log predictive error the optimum committee was determined using the validation error. The test errors of the ten committees are given in Table 9 and Fig. 17 shows the test

**Table 7 Variables used in analysis of elongation**

| Variable | Range | Mean | Standard deviation |
|---|---|---|---|
| Chromium, wt-% | 13–20 | 17·45 | 3·19 |
| Aluminium, wt-% | 0–4·5 | 2·74 | 2·20 |
| Titanium, wt-% | 0·5–3·50 | 1·02 | 0·86 |
| Molybdenum, wt-% | 0–1·5 | 0·35 | 0·58 |
| Yttria, wt-% | 0–0·5 | 0·42 | 0·15 |
| Recrystallisation temperature, °C | 20–1330 | 729 | 585 |
| Recrystallisation time, s | 0–120 | 28·92 | 33·72 |
| Aging temperature, °C | 20–800 | 171 | 309 |
| Aging time, s | 0–2888 | 354·8 | 778 |
| Cold work, % | 0–70 | 11·4 | 22·59 |
| Test temperature, °C | 0–1250 | 561·4 | 340·2 |
| Strain rate, $s^{-1}$ | $3 \times 10^{-8}$–$3 \times 10^{-2}$ | $1{\cdot}3 \times 10^{-3}$ | $2{\cdot}7 \times 10^{-3}$ |
| UTS, MPa | 70·7–1680 | 545 | 390 |
| Yield strength, MPa | 63–1600 | 468 | 367 |
| Elongation, % | 0·8–49·29 | 12·13 | 8·18 |

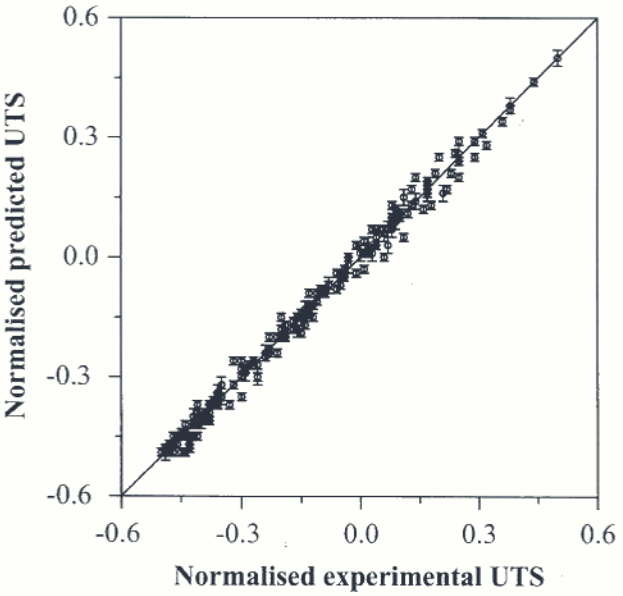


**14 Normalised predicted ultimate tensile strength versus normalised experimental results for whole data set after retraining using optimum committee**

error versus ranking for the best models, and the test errors of the committees.

As shown in Fig. 17*b* the committee consisting of the top six models shows the least test error and was therefore selected as the optimum model. Figure 18 shows the plots of the predicted values versus experimental values for the single best model and the committee. The plot for the committee after retraining the committee models using the whole data set is shown in Fig. 19.

Figure 20 shows the plot of the model perceived significance of the variables $\sigma_v$ for the six models contained in the committee. Test temperature can be seen to have a marked effect on elongation. This is expected and it is exciting to note the consistency with the patterns shown in the yield and ultimate strength models. The perceived influence of yield strength on elongation is slightly greater than that of ultimate tensile strength on elongation. This is expected metallurgically since it is the difference between the yield strength and UTS that relates to the uniform component of elongation.

**Table 8 Ranking by log predictive error for 10 best models of elongation**

| Ranking | Hidden units | Seed | Test error | Log predictive error |
|---|---|---|---|---|
| 1 | 14 | 50 | 0·17988 | 161·23 |
| 2 | 14 | 30 | 0·19329 | 160·86 |
| 3 | 11 | 30 | 0·21316 | 159·76 |
| 4 | 13 | 50 | 0·20960 | 159·47 |
| 5 | 8 | 100 | 0·19966 | 158·05 |
| 6 | 7 | 50 | 0·18807 | 157·47 |
| 7 | 5 | 100 | 0·21390 | 156·42 |
| 8 | 4 | 30 | 0·21008 | 155·44 |
| 9 | 10 | 100 | 0·20382 | 155·81 |
| 10 | 10 | 10 | 0·20522 | 154·51 |

**Table 9 Test errors of committees organised for estimation of percentage elongation: note that test error of best committee is less than that of single best model**

| Model in committee | Test error |
|---|---|
| 1 | 0·17987 |
| 2 | 0·17642 |
| 3 | 0·17930 |
| 4 | 0·17921 |
| 5 | 0·18035 |
| 6 | 0·17368 |
| 7 | 0·17504 |
| 8 | 0·17702 |
| 9 | 0·17639 |
| 10 | 0·17726 |

## Application of models

Attempts were made to use the committee models to predict the influence of the variables on the ultimate tensile strength, yield strength, and percentage elongation of the iron base MA-ODS alloys and to determine whether the perceived relationships are reasonable from the point of view of the established metallurgical information. All the

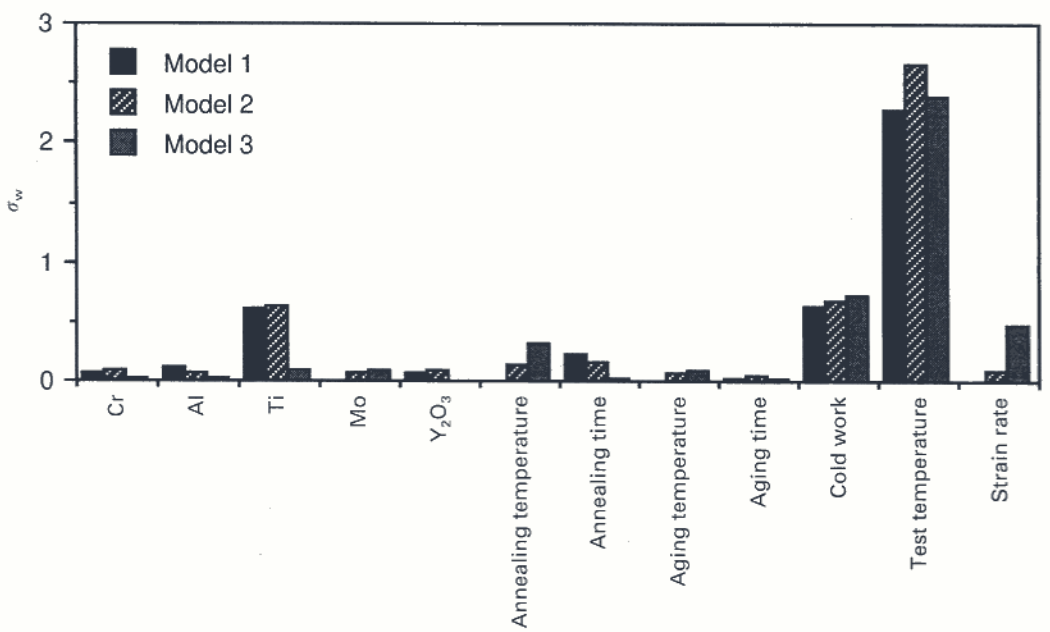


**15 Model perceived significance of input parameters for committee model trained on all ultimate tensile strength data: $\sigma_w$ values for all members of committee are presented for each variable**

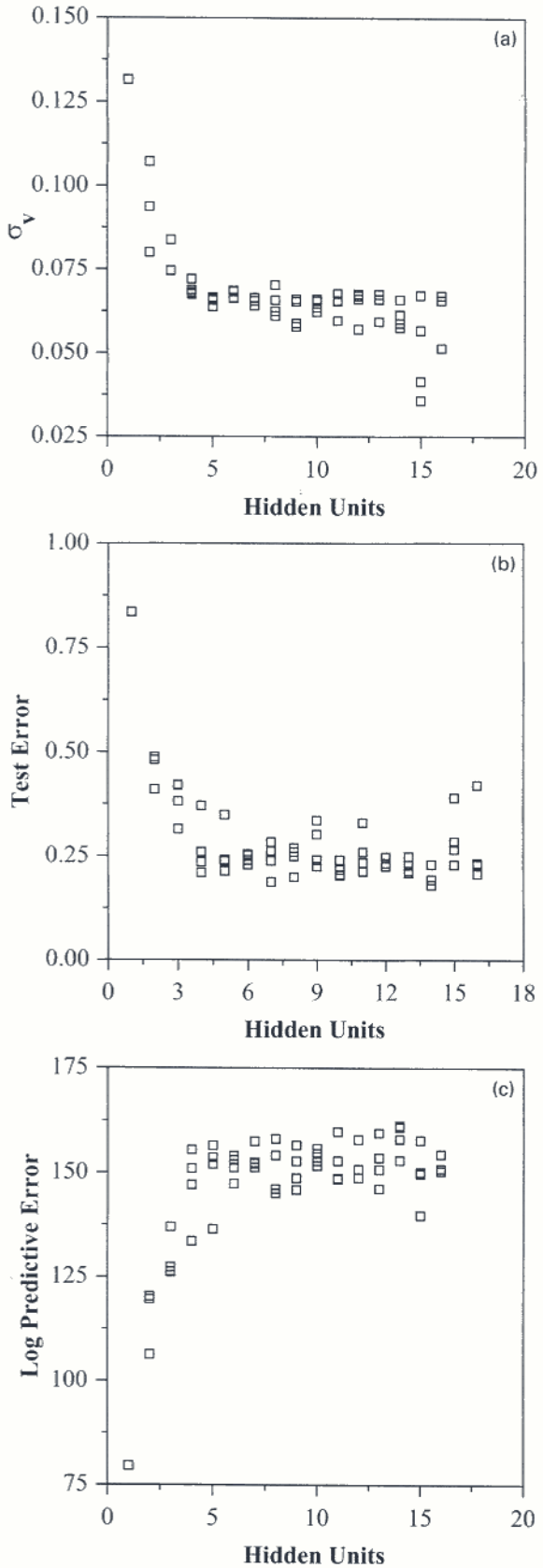


**16 Percentage elongation analysis: variation in *a* model perceived noise level $\sigma_v$, *b* test error, and *c* log predictive error as functions of number of hidden units (i.e. complexity of model) – several values are presented for each set of hidden units because training for each network was started with various random seeds (note that higher value of log predictive error in *c* indicates superior model)**

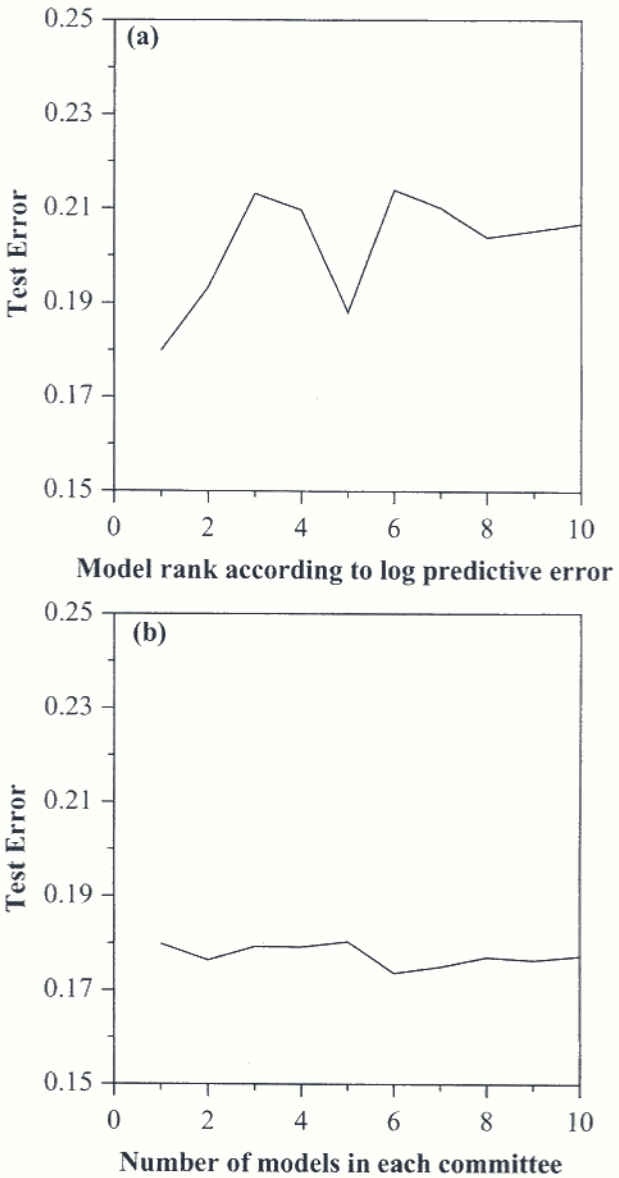


**17 *a* test errors of top 10 elongation models and *b* corresponding test errors for committees of models**

results are presented along with the $\pm 1$ standard deviation predicted error bars.

## EFFECT OF TEMPERATURE

Figure 21 shows the predicted effect of test temperature on the yield strength, ultimate strength, and elongation of MA956 for both recrystallised and unrecrystallised conditions.

The predicted patterns are fairly reasonable. There is no significant reduction in strength until about 500°C. Similarly, there is no noticeable change in elongation until the region corresponding precisely to the decrease in strength, when the elongation increases. This is consistent with the established property that increasing temperature leads to a decrease in strength and an increase in elongation. However, the sharp decrease in strength and corresponding sharp increase in elongation is peculiar although well known.[9,10] An explanation that the sharp changes occur at a temperature where the dislocation density is effectively reduced would have been appropriate had the pattern not been the same for both the recrystallised and unrecrystallised conditions. It may be that dislocation climb over the fine yttria particles becomes prominent in the regime where the sharp reduction is observed. The alloy can be seen to show higher

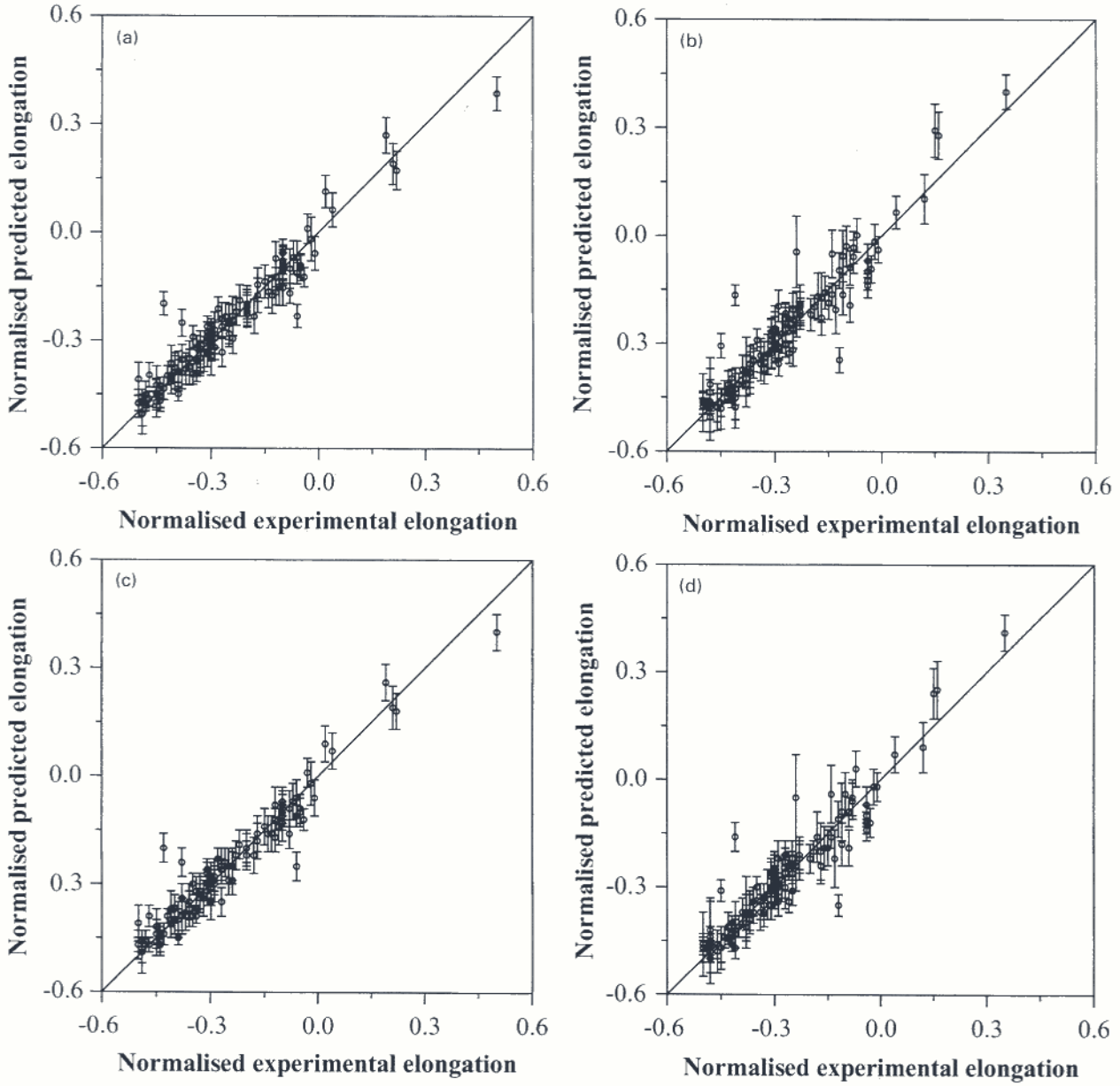


*a* single model, training data set; *b* single model, test data set; *c* committee, training data set; *d* committee, test data set

**18 Normalised predicted percentage elongation versus normalised experimental results using *a*, *b* single best model and *c*, *d* optimum committee**

percentage elongation in the unrecrystallised condition than when recrystallised. This seems unusual as the alloys in the unrecrystallised condition are harder and would be expected to be less ductile. However, this result is consistent with extensive experimental work by Alamo *et al.*[10] which indicates that it is the coarse columnar grain structure which leads to poor ductility in the recrystallised alloys.

The experimental strengths and percentage elongations of the various commercial MA-ODS ferritic steels are compared in Fig. 22. The heat treatment conditions of the alloys are as for commercial applications. The DT and DY alloys are subjected to an aging treatment to precipitate $\chi$ phase for higher strength. This effect is correctly predicted, with higher ultimate strength for DT and DY than for MA956 which contains no $\chi$ phase. The DY alloy contains yttria particles whereas DT does not, and this explains the higher strength of DY compared with DT. As can be seen the yield strength of MA956 is higher than that of DT despite the presence of $\chi$ phase in the latter. This is because of the yttria particles in MA956 and clearly demonstrates that the effect of dispersoid strengthening is primarily on the yield strength rather than on the ultimate strength. The plots of percentage elongation further demonstrate the effects of dispersoids, with DT showing greater ductility because yttria particles are not present. It can then be summarised that yttria particles increase yield strength and reduce ductility and that the lower ductility in DY, in which both $\chi$ phase and yttria particles are present, occurs as a result of the yttria particles.

## EFFECT OF TITANIUM, MOLYBDENUM, AND YTTRIA CONTENT

Figure 23 shows the effects of titanium, yttria, and molybdenum on the yield strength, ultimate strength, and elongation of MA956. The ultimate strength and yield strength increase with titanium content; elongation, however, appears insensitive. The increase in strength with increasing titanium is generally thought to occur via $\chi$ phase but this is not formed in MA956, in which the titanium has a solid solution strengthening effect, thus affecting both the ultimate and yield strength almost equally. The effect of

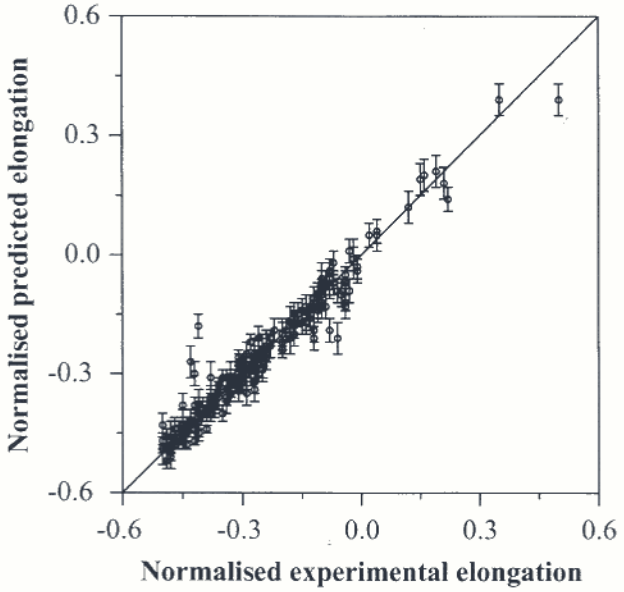


**19 Normalised predicted percentage elongation versus normalised experimental results for whole data set after retraining using optimum committee**

yttria content is slightly more pronounced on the yield strength than the ultimate tensile strength, although the error bars are large. The bar charts of the model perceived significance of variables for the yield strength and ultimate strength in Figs. 9 and 15 respectively show a stronger yttria effect for the yield strength than the ultimate strength, in agreement with the above observations. The results of an experimental work by Kawasaki *et al.*[26] on the effect of dispersoids on tensile deformation of Fe–20Cr oxide dispersion strengthened alloys has helped to establish the reliability of the predicted patterns. Addition of yttria particles was reported[26] to increase the 0·2% yield stress over the entire experimental temperature range (300–1073 K), and at temperatures higher than 673 K the increment of work hardening due to the dispersoids was found to be small. The ultimate tensile strength is a function of work hardening and this probably explains why the predicted effect of dispersoids on the ultimate tensile strength is generally less pronounced than for the yield strength. These predicted types of behaviour with respect to titanium and yttria concentrations are significant as they seem to corroborate the explanation given above for the predicted tensile properties of the different MA-ODS steels. Titanium, through $\chi$ phase, is responsible for the higher ultimate strength of DT and DY compared with MA956. The higher yield strength for MA956 than for DT and the higher ductility of DT compared with MA956 and DY are because of the yttria particles in MA956 and DY. Strength and elongation are shown to be insensitive to molybdenum content in MA956. Apart from providing solid solution strengthening, molybdenum is a constituent in $\chi$ phase and as such increasing its concentration is expected to contribute positively to strength. However, $\chi$ phase formation depends on the titanium concentration, which is very low in MA956; an increase in the molybdenum concentration may not, therefore, have any any effect. The model seems to have recognised correct patterns.

## EFFECT OF CHROMIUM AND ALUMINIUM

The predicted effects of chromium and aluminium on the tensile properties of MA956 are shown in Fig. 24. Changes in concentration have negligible effects on the strength and elongation of MA956. However, the error bars are so large that it is not possible to reach a satisfactory conclusion. Large error bars occur as a result of either noisy data or sparse data. It is suspected that both of these factors are responsible for the absence of a significant relationship for chromium or aluminium.

## EFFECTS OF RECRYSTALLISATION TEMPERATURE AND TIME

The effects of the recrystallisation temperature and recrystallisation time on the yield strength, ultimate strength, and elongation are shown in Fig. 25. As expected the ultimate strength decreases with increasing recrystallisation temperature or time. The yield strength seems insensitive to the recrystallisation temperature. The elongation shows a significant increase with the recrystallisation temperature.

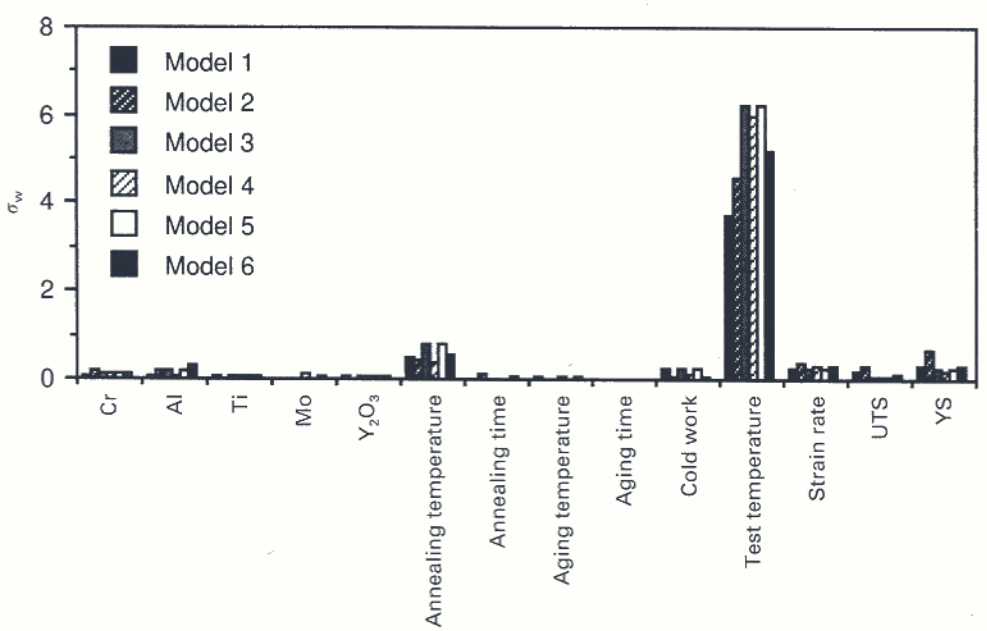


**20 Model perceived significance of input parameters for committee model trained on all percentage elongation data: $\sigma_w$ values for all members of committee are presented for each variable**

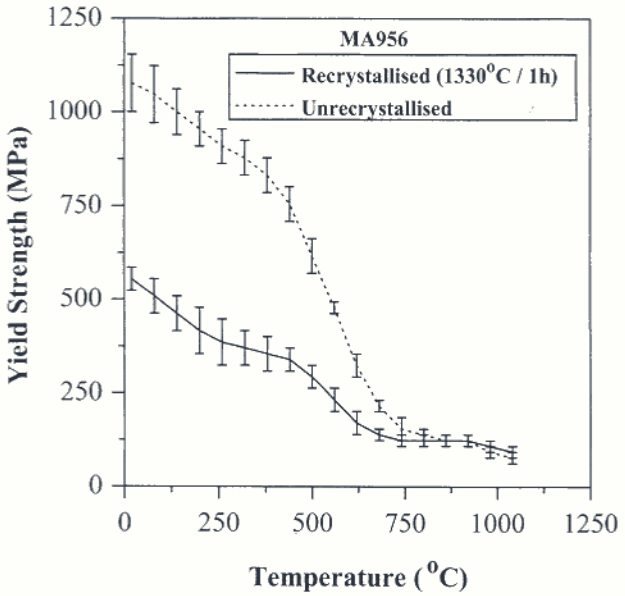


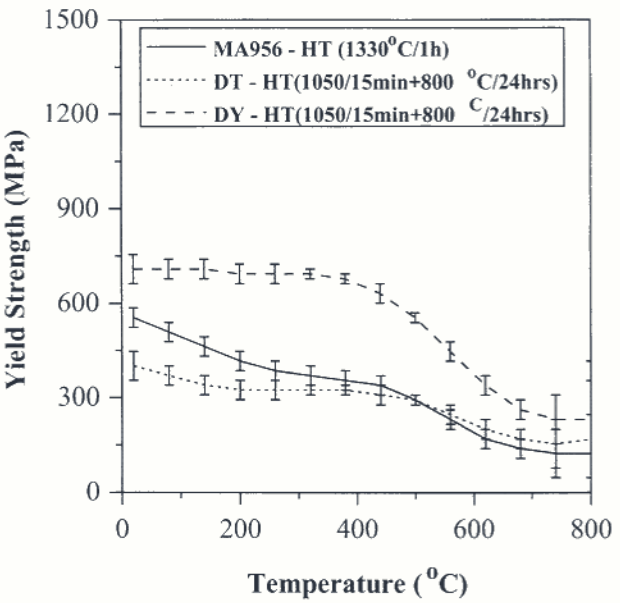


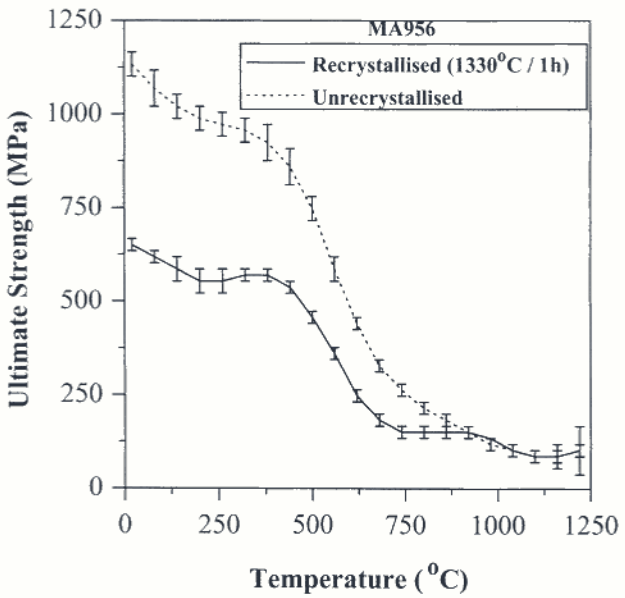


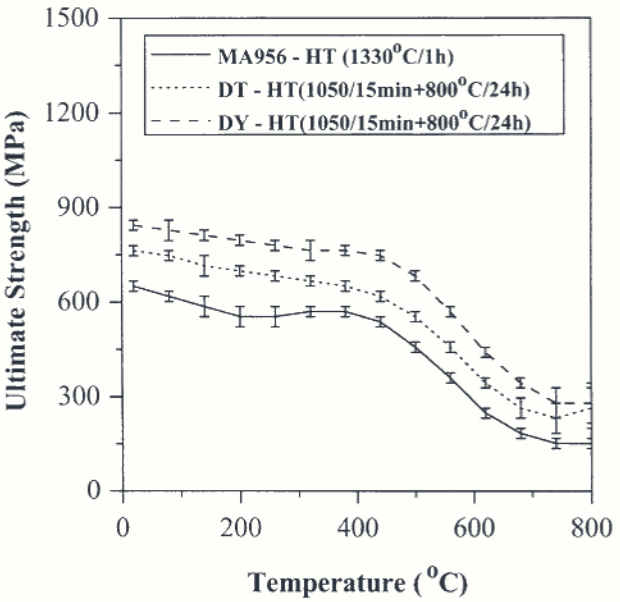


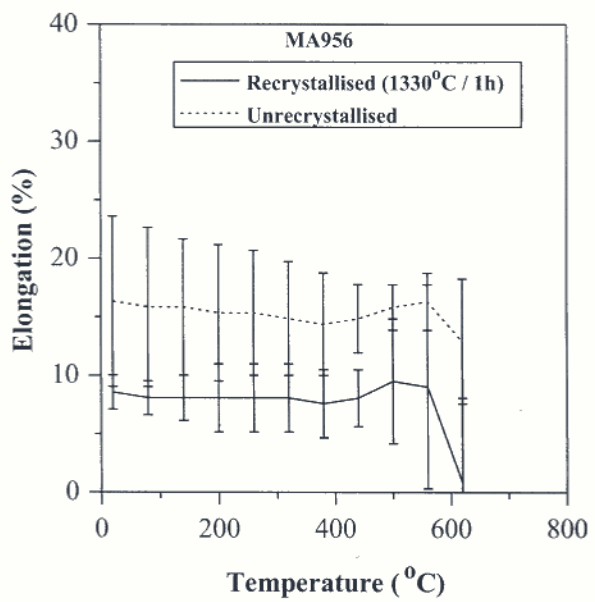


21 Effect of temperature on yield strength, ultimate tensile strength, and percentage elongation of MA956

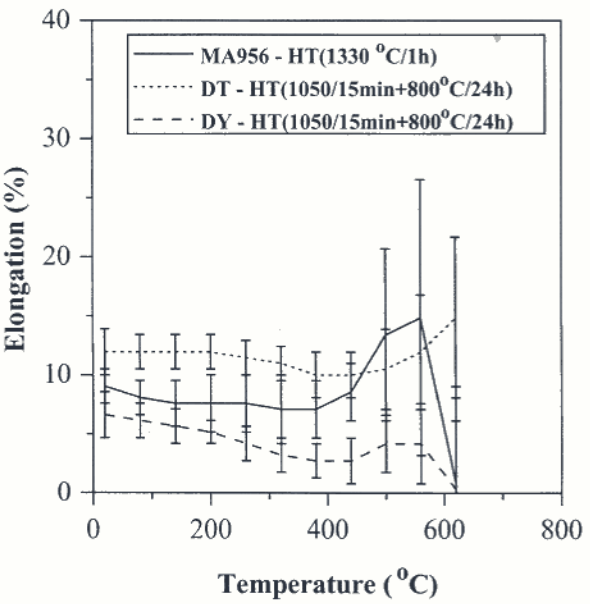


22 Comparison of predicted properties of some MAODS ferritic steels

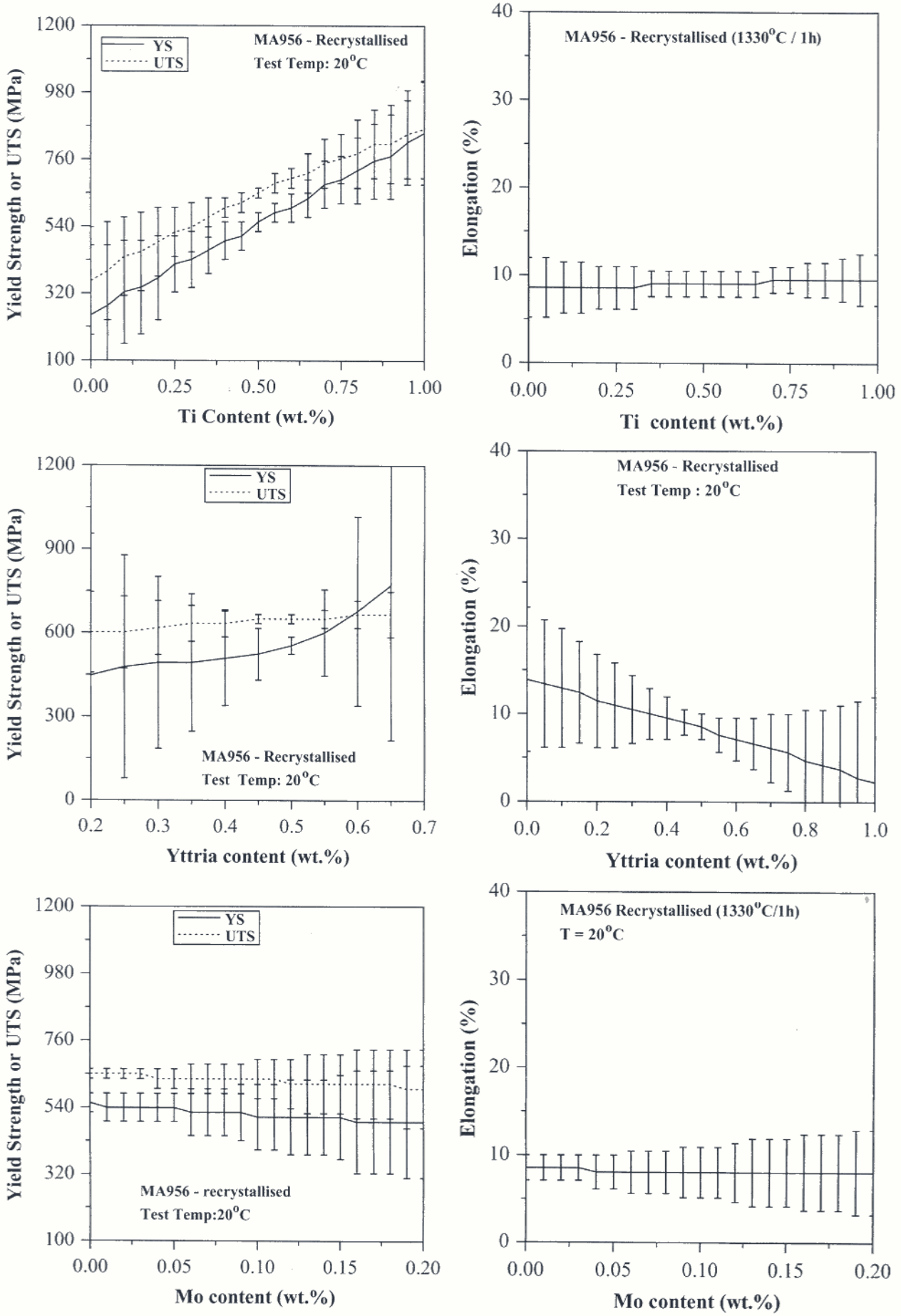


**23 Predicted effect of titanium, yttria, and molybdenum on yield strength, ultimate strength, and percentage elongation of MA956**

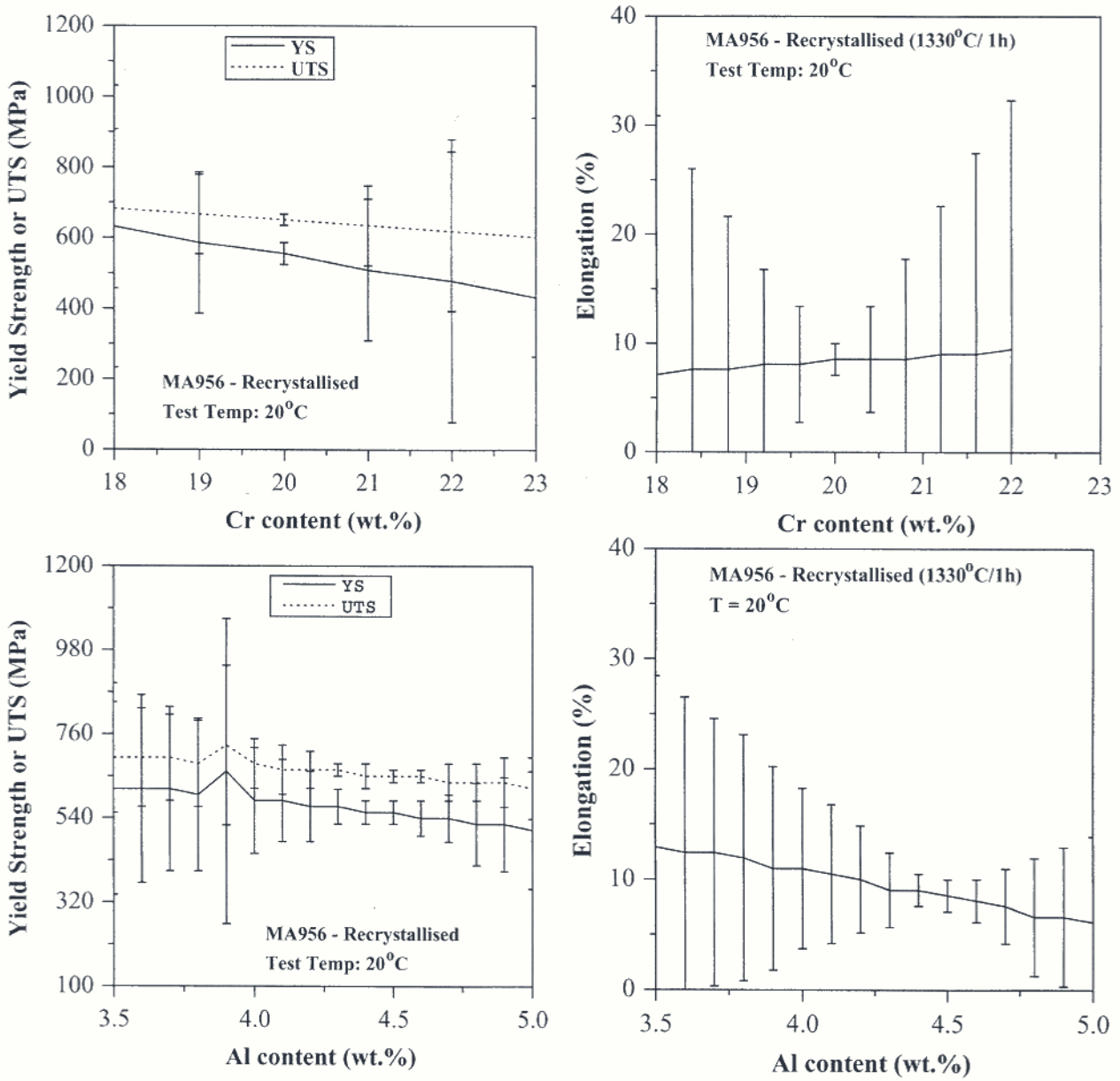


**24 Predicted effect of chromium and aluminium on yield strength, ultimate tensile strength, and percentage elongation of MA956**

## EFFECTS OF COLD WORK AND STRAIN RATE

Figure 26 shows the predicted effects of cold work and strain rate on the ultimate strength, yield strength, and elongation of MA956. As expected, increasing cold work increases the ultimate strength and the yield strength and a saturation level is predicted above which further cold work does not lead to an increase in strength. Although the error bars are large for the elongation, the predicted pattern is that expected, showing decreasing ductility with increasing cold work. The large error bar is due to the very limited number of examples where cold work is varied in the database. The strength and elongation are found to be insensitive to low strain rate, but at high strain rate the strengths increase and elongation decreases accordingly with increasing strain rate. These results are in excellent agreement with published experimental work.[27]

## Summary

Tensile property data for mechanically alloyed, oxide dispersion strengthened ferritic stainless steels have been analysed using a neural network technique within a Bayesian framework. The analysis, although empirical, can after appropriate training and with the use of a committee of models produce results which are metallurgically reasonable.

The present authors' experience of the neural network method suggests that it has considerable potential for useful applications in materials science. It is particularly useful in circumstances where there is extreme complexity, such that physical models can not be constructed within a reasonable timescale.

Neural networks are frequently used for regression problems in which continuous variables are modelled. They can also be applied to classification problems where the variables to be predicted adopt discrete values.[28]

The technique is extremely powerful; it can in principle produce a model for a random set of points. There are many models available, for example, on the worldwide web or from commercial sources. Care must however be taken to select those which incorporate an effective strategy for avoiding the problem of overfitting the data. Methods in which the error bar depends on the position in the input space are particularly reliable.

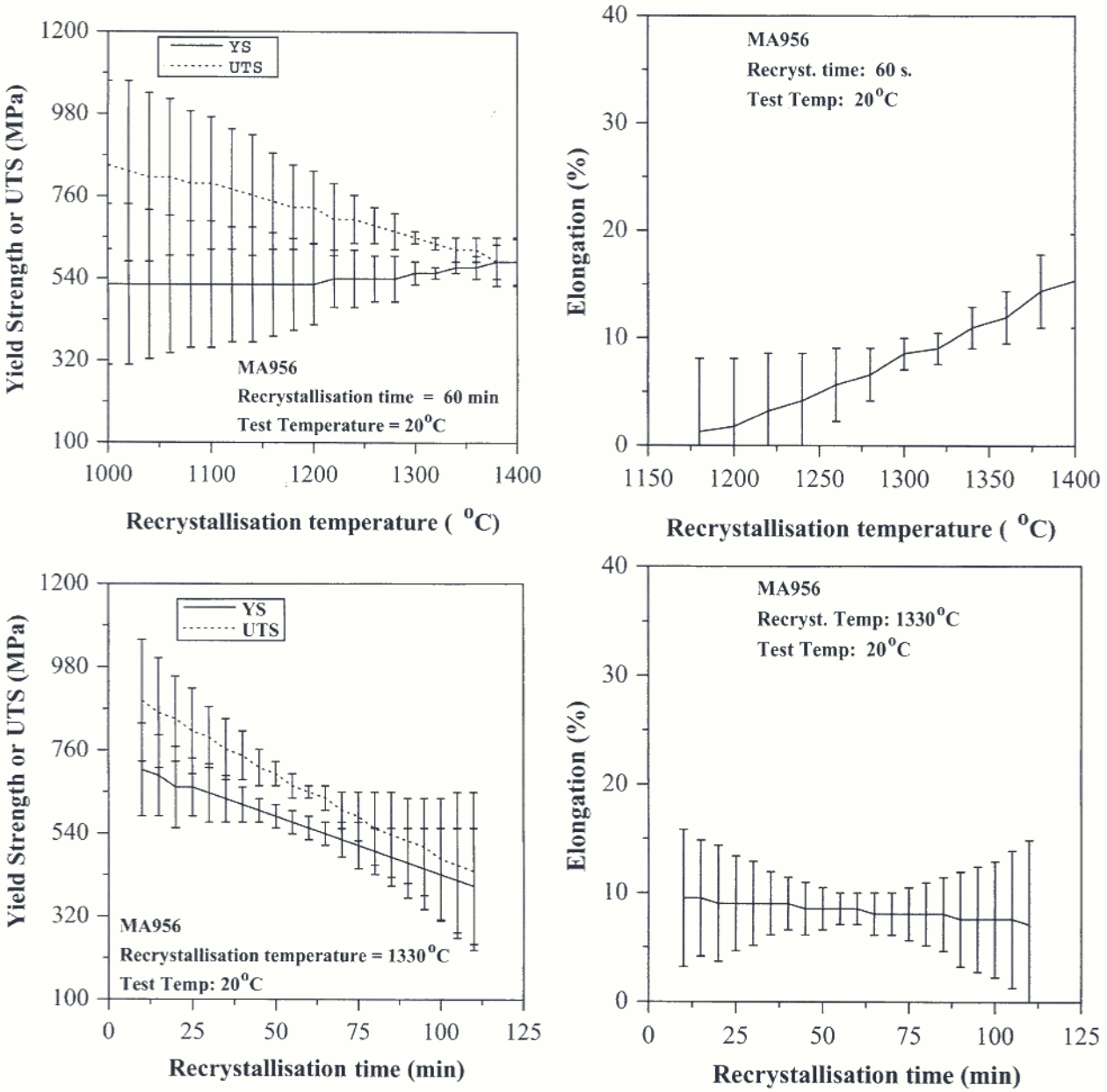


**25 Effects of recrystallisation temperature and recrystallisation time on tensile properties of MA956**

Finally, the neural network, like all regression methods, is a purely mathematical tool which cannot necessarily distinguish between cause and effect. The selection of appropriate inputs and outputs is important in deducing physically sound relationships.

## Acknowledgements

The authors are grateful to Inco Alloy Limited, Hereford, UK for its various contributions in terms of both materials and useful suggestions by the representatives of the Research and Development Department at three-monthly technical discussions. Data provided by Dr A. R. Jones, Liverpool University, UK are also gratefully acknowledged. The authors are grateful to Professor A. Windle for the provision of laboratory facilities at the University of Cambridge. One of the authors (AYB) would like to acknowledge the financial support of the Cambridge Commonwealth Trust and the Association of Vice-Chancellors and Principals of Universities and Colleges in the UK for an Overseas Research Studentship.

## References

1. J. S. BENJAMIN: *Metall. Trans.*, 1970, **1**, 2943.
2. D. E. RUMELHART, G. E. HINTON, and R. J. WILLIAMS: *Nature*, 1986, **323**, 533–536.
3. INCOMAP: Incoloy alloy MA956 (information sheet), Inco Alloys, Hereford, UK.
4. J. D. WHITTENBERGER: *Metall. Trans.*, 1981, **12A**, 845–851.
5. R. J. SALOMON: *J. Phys. (France) IV*, 1993, **C7–III**, 697–702.
6. C. ZAKINE, C. PRIOUL, A. ALAMO, and D. FRANCOIS: *J. Phys. (France) IV*, 1993, **C7–III**, 591–596.
7. B. DUBIEL, W. OSUCH, M. WROBEL, A. CZYRSKA-FILEMONOWICZ, and P. J. ENNIS: in 'Materials for advanced power engineering', Part 2, 1523–1532; 1994, Dordrecht, The Netherlands, Kluwer Academic Publishers.
8. W. HENDRIX and W. VANDERMEULEN: BLG 557 information sheet, SCK/CEN, Mol, Belgium, 1982.

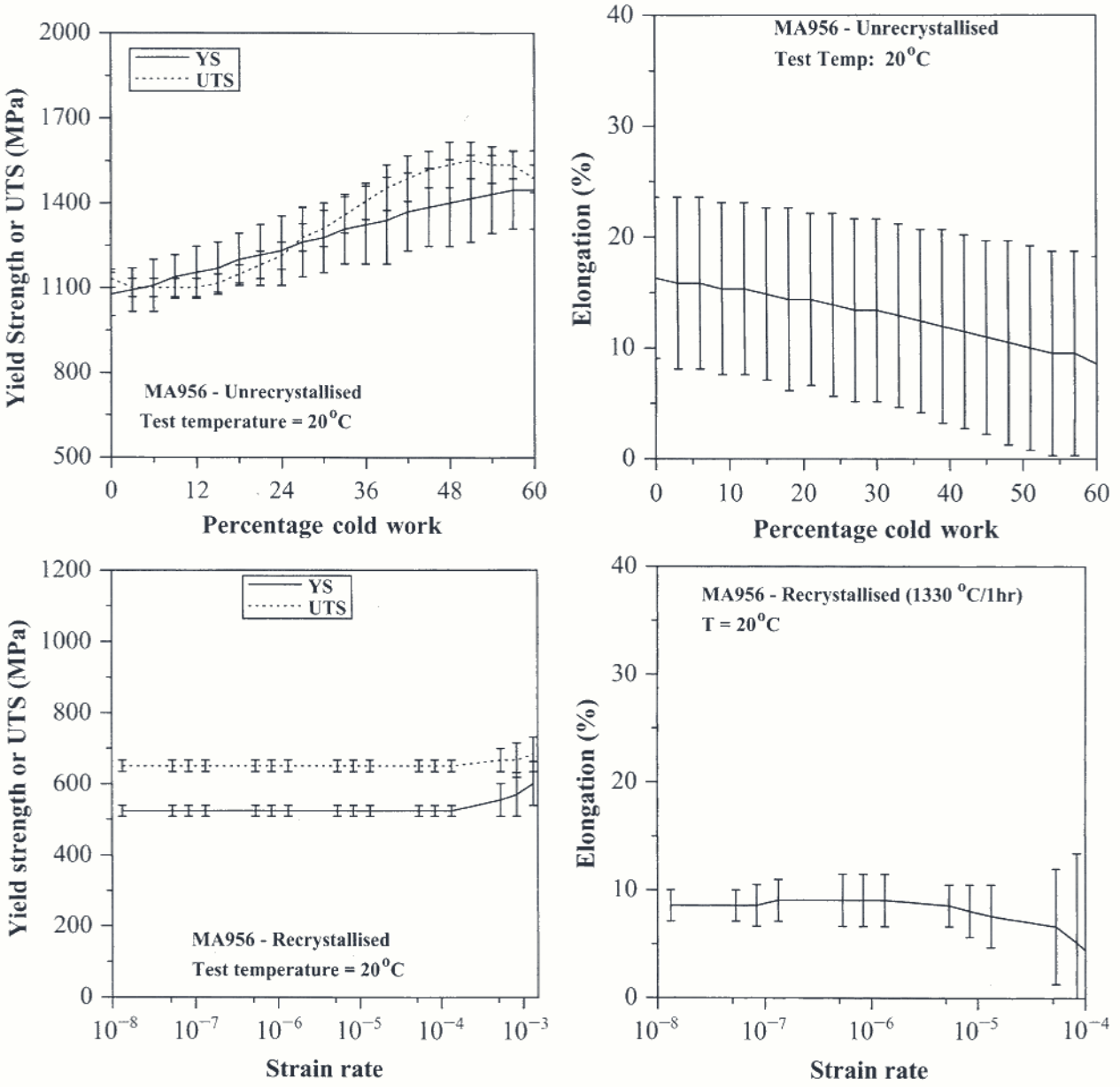


**26 Effects of cold work and strain rate on tensile properties of MA956**


9. A. ALAMO, J. DECOURS, M. PIGOURY, and C. FOUCHER: in Proc. Conf. on 'Structural applications of mechanical alloying', Myrtle Beach, SC, March 1990, 89–98; 1990, Materials Park, OH, ASM International.
10. A. ALAMO, H. REGLE, and J. L. BECHADE: *Novel Powder Process. Met. Powder Ind. Fed. Princeton NJ*, 1992, **1**, 169.
11. H. REGLE: PhD thesis, Université de Paris, France, 1994.
12. D. J. C. MACKAY: *Neural Comput.*, 1992, **4**, 415–447.
13. D. J. C. MACKAY: *Neural Comput.*, 1992, **4**, 448–472.
14. D. J. C. MACKAY: *Network: Comput. Neural Systems*, 1995, **6**, 469–505.
15. D. J. C. MACKAY: *Trans. Am. Soc. Heat. Refrig. Air-Cond. Eng.*, 1994, **100**, 1053–1062.
16. D. J. C. MACKAY: in 'Mathematical modelling of weld phenomena 3', (ed. H. Cerjak and H. K. D. H. Bhadeshia), 359–389; 1997, London, The Institute of Materials.
17. H. K. D. H. BHADESHIA, D. J. C. MACKAY, and L.-E. SVENSSON: *Mater. Sci. Technol.*, 1995, **11**, (10), 1046–1051.
18. J. JONES and D. J. C. MACKAY: in Proc. 'Superalloys '96', 417–424; 1996, Warrendale, PA, TMS.
19. L. GAVARD, H. K. D. H. BHADESHIA, D. J. C. MACKAY, and S. SUZUKI: *Mater. Sci. Technol.*, 1996, **12**, (6), 453–463.
20. T. COOL, H. K. D. H. BHADESHIA, and D. J. C. MACKAY: *Mater. Sci. Eng. A*, 1997, **A223**, (1–2), 186–200.
21. H. FUJII, D. J. C. MACKAY, and H. K. D. H. BHADESHIA: *ISIJ Int.*, 1996, **36**, 1373–1382.
22. T. COOL and H. K. D. H. BHADESHIA: in 'Mathematical modelling of weld phenomena 3', (ed. H. Cerjak and H. K. D. H. Bhadeshia), 403; 1997, London, The Institute of Materials.
23. W. G. VERMEULEN, P. F. MORRIS, A. P. de WEIJER, and S. van der ZWAAG: *Ironmaking Steelmaking*, 1996, **23**, (5), 433–437.
24. W. G. VERMEULEN, S. van der ZWAAG, P. F. MORRIS, and T. de WEIJER: *Steel Res.*, 1997, **68**, 72–79.
25. W. G. VERMEULEN, A. BODIN, and S. van der ZWAAG: *Steel Res.*, 1997, **68**, 20–26.
26. Y. KAWASAKI, Y. IKEDA, T. KOBAYASHI, and H. SUMIYOSHI: *ISIJ Int.*, 1996, **36**, 1208–1214.
27. J. D. WHITTENBERGER: *Metall. Trans.*, 1979, **10A**, 1285.
28. K. ICHIKAWA, H. K. D. H. BHADESHIA, and D. J. C. MACKAY: *Sci. Technol. Weld. Joining*, 1996, **1**, (1), 43–50.